A 3D finite element method for flexible multibody systems

Johannes Gerstmayr, Joachim Schöberl

18th May 2004

Abstract

An efficient finite element (FE) formulation for the simulation of multibody systems is derived from Hamilton's principle. According to the classical assumptions of multibody systems, a large rotation formulation has been chosen, where large rotations and large displacements, but only small deformations of the single bodies are taken into account. Absolute coordinates are chosen for the degrees of freedom. The numerical solution strategy is based on the assumption that the period of large rotations of the single bodies is much larger than the period of oscillations due to deformation. The strain tensor is modified based on the latter assumption and therefore, the present formulation distinguishes significantly from standard nodal based nonlinear finite element methods. Constraints are defined in integral form for every pair of surfaces of two bodies. This leads to a small number of constraint equations and avoids artificial stress singularities. Due to the special structure of the resulting system, the most expensive part of the system of equations can be solved in advance and only once for a given Runge-Kutta scheme. The present method has been implemented and tested with the FE-package NETGEN/NGSOLVE.

Keywords: absolute coordinate formulation, large rotation theory, finite elements, time–integration

1 Introduction

The dynamics of mechanical systems including large deformations normally leads to a nonlinear stiffness matrix, see Zienkiewicz and Taylor [34]. In conventional geometrically nonlinear finite element (FE) formulations, the stiffness matrix has to be updated frequently within Newton's method and is therefore computationally costly. It shall be emphasized that the specific aim of the present formulation is to simulate mechanical problems with large displacements but small deformations, which means small strain as well as small displacements with respect to a co-rotated reference frame. It is obvious that due to this special assumptions the strategy can be more efficient compared to standard nonlinear finite element methods. This is applicable for the case for several engineering applications, like a gear unit or a crankshaft.

Multibody system dynamics has developed to a stand-alone field of research in the past decades and several books emerged, among them [5, 10, 20, 21, 23, 24, 27, 28, 29, 33]. Starting with rigid-body dynamics, the equations of motion can be derived e.g. from Lagrange's equations. Including the flexibility of single bodies, simplified formulations like beam theory have reached large importance in multibody dynamics, e.g. for the investigation of a slider-crank mechanism [9], the stability of a rotor-blade of a helicopter or the stability of a satellite with highly flexible solar panels, see Bremer [5]. While most of these approaches use the conventional beam-theory with respect to a moving frame, Simo derived a newer approach based on the large rotation vector, see Simo and Vu-Quoc [32]. Shabana summarized different methods for the modeling of multibody systems in his book [27]. He proposes a floating frame of reference formulation (FFRF) for the modeling of multibody systems and treats numerous examples. In the case of structural elements, the FFRF is advantageous because the elastic deformation can be described easier in the corotated reference frame than in a global frame.

In the case of solid 2D and 3D flexible multibodies, the number of possible formulations is much lower than for structural multibodies. Two main formulations are well known. The first one is based on geometrically nonlinear FE. It results in a constant mass matrix and a nonlinear stiffness matrix. Standard FE codes which include geometrically nonlinear behavior are mostly based on such formulations, the solution differs between the so-called total and updated Lagrangian formulation. A formulation which is based on the co-rotational approach and the updated Lagrangian formulation has been introduced by Pan and Haug [26]. In the case of multibody systems, the geometrically nonlinear FE formulation is coupled with possibly nonlinear constraints and the resulting formulation is therefore sometimes called absolute coordinate formulation (ACF), see e.g. Kübler et al. [22]. This term may not be mixed up with absolute nodal coordinate formulation (ANCF), which is a special formulation for flexible multibody dynamics. There, absolute coordinates represent slopes and displacements of nodes. The second approach is based on the FFRF. There, it is possible to utilize all the knowledge from small strain theory because the linear equations of motion for a single body without rigid body motion are nonlinearly transformed by means of the rigid body rotation of the corotated reference frame. E.g. Ambrósio [1] combines the FFRF and standard FE methods and derives a formulation which can treat physical nonlinearities like plasticity. However, the coupling of small deformations and large rotations leads to complex nonlinear terms in the mass matrix which then has to be re-computed in every time step. Only few publications on solid 2D or 3D flexible multibody systems can be found in the open literature. Simeon [31] uses stabilization techniques in order to solve a solid 2D flexible multibody systems with contact. Eberhard [8] introduces a hybrid FE and multibody method and switches between rigid and elastic behavior of the bodies depending on the state of the bodies. Orden [25] uses the geometrically nonlinear FE method to discretize his models and applies the energy-momentum method in order to get a stable integration.

In the past decade, engineering problems from industry led to a further development of the well known component mode synthesis based on Craig-Bampton modes, for details on the formulation with multibody systems see Géradin and Cardona [10]. In the case of the FFRF, the possibly large number of degrees of freedom of a FE mesh is reduced by means of a modal decomposition of the original mesh. The modal decomposition works well for the FFRF, because of the linearity with respect to the corotated reference frame. The approximation with a small number of eigenmodes compared to the original degrees of freedom turns out to converge fast if all static modes are included. One possible drawback of this method is the necessary

modal analysis in the preprocessing, which is nowadays possible for very complex meshes due to efficient numerical solvers for eigenvalue problems. Another problem arises, if the number of boundary and constraint conditions leads to a large number of static modes, which reduces the performance of the numerical solution. For the reduced problem, a highly nonlinear system of equations of motion has to be solved. Due to the fact that modal synthesis is based on a linear decomposition, it is primarily not suitable for physically or geometrically nonlinear problems. However, some experiments have been made for beam-type multibody systems with eigenmodes and plasticity, see Gerstmayr and Irschik [12, 11].

The present approach for 3D multibody systems is based on geometrically nonlinear FE methods. The new feature of this method is the decomposition of the strain into a small deformation and a large rotation, which is especially adapted to flexible multibody systems. Unlike many existing multibody dynamics formulations we use absolute coordinates and no rotational degrees of freedom in order to get a constant mass matrix and a nonlinear stiffness matrix. In contrast to the co-rotational FE approach of Argyris [2] or Belytschko [3], the large rotation is equal for all elements of a single body, the decomposition of the rotation is different and only small deformations are permitted in the present approach. It turns out in the discretized form of the equations of motion that the nonlinear stiffness matrix can be replaced by means of the constant small strain stiffness matrix which undergoes an orthogonal transformation by means of the nonlinear rotation matrix. Additionally there is a nonlinear part of quadratic terms of the small deformation quantities, which turns out to be of lower significance in the solution strategy. While it has been shown, that the present formulation can be transformed into the FFRF by means of a coordinate transformation, see Gerstmayr [14], the solution strategy within an implicit time–integration method shows significant advantages compared to the FFRF. Due to the assumption that rigid body rotations change slowly within one time step, the nonlinear stiffness matrix can be approximated by means of the small strain stiffness matrix transformed by the rotation matrices of the single bodies computed from the last time step. A small number of iterations (between two and four) for the solution of the nonlinear equations within a single time step shows that the approximated nonlinear stiffness matrix contains the main terms. The method can be compared to the concept of the modified Newton's method, where the Jacobian of the method is computed during the last iteration. The significant advantage of the present method lies in the efficient computation of the inverse of the Jacobian, because no large systems of equations has to be factorized. The Jacobian is computed by means of application of the rigid body rotation matrices to the mass matrix times the inverse of the small strain stiffness matrices.

For the numerical time–integration, higher order implicit Runge Kutta methods have been implemented. For dynamical problems, solution methods differ between explicit and implicit methods. In explicit methods, only the factorization of the mass matrix is necessary, while the so-called elastic forces only need to be evaluated. The schemes are computationally cheap for one time step, but stability criteria require a small time step depending on the highest eigen-frequences. For the special case of differential algebraic equations (DAEs), explicit methods are unstable in general, independent of the time step. Certain implicit schemes, like special Lobatto or Radau classes, see Hairer et al. [19], are stable independent of the time step for the case of ordinary differential equations, and are stable for the case of specific classes of DAEs. However, implicit methods require the solution of a nonlinear system of equations and lead to a Jacobian which is decomposed of a constant mass matrix and a non-constant stiffness matrix. For large deformation problems, e.g. the bending of an initially straight beam into a circle, there is a significant difference between the Jacobian for initial values (straight beam) and the Jacobian for the final state (curved beam) such that the computation has to be performed stepwise and several Jacobians need to be computed. In the case of large displacements (including large rotations) but small deformations, the Jacobian undergoes significant changes, too, but a detailed investigation shows that the underlying rigid body rotation is mostly influencing the non-constant part of the Jacobian. In the present contribution multibody systems are considered, where high-frequency deformation is coupled to low-frequency rigid-body rotations of the single bodies. The strain tensor, which is used for the computation of the strain energy as well as for the stiffness matrix, is modified such that only linear dependence on small deformations coupled nonlinearly with rigid body rotations are considered. For details with respect to accuracy and stability of such methods, see e.g. Hairer et al. [19, 17, 18]. In a resent work on implicit Runge Kutta methods for the present ACF, a n-stage Runge Kutta formula is used to integrate the equations of motion directly, see Gerstmayr and Schöberl [16]. In that

case, a larger matrix containing the mass matrix and the small strain stiffness matrix has to be factorized in the preprocessing phase. In the present paper, one-step methods are used to approximate the stages of a n-stage Runge-Kutta formula and iterated till the residual of the n-stage formula is practically zero. This strategy avoids the computation of larger systems of nonlinear equations for every time step. The present method turns out to work well with linear constraints. The method has been extended for the case of non-linear material behavior, see Gerstmayr [13].
The paper is organized as follows: Section 2 includes a brief derivation of the equations of motion and the definition of the reduced strain measure. Section 3 presents the decomposition of the total displacement of a point into a rigid body part and a small deformation. In Section 4, constraint equations modeled by means of distributed constraints are introduced through the limit case of the penalty method which leads to the Lagrange multiplier technique. Section 5 shows the equations of motion with a detailed analysis of the variation of the reduced Green strain measure. The equations of motion are discretized in Section 6 and a time–integration scheme is applied exemplarily in Section 7. In Section 8 and 9 two examples are presented which show the accordance of the formulation with standard FFRF beam-type formulations. While differences could be expected due to differences of the 3D solid model and the beam theory due to special supports of the 3D structure and due to the non-symmetry of the tetrahedral mesh, both formulations turn out to coincide perfectly. Furthermore, the examples show that the use of integral constraints is comparable to constraints in structural elements. It shall be emphasized that the implementation has not been optimized and therefore computational times are not comparable to those of commercial software. The advantages of the formulation are documented in its outstanding appearance of the equations of motion. Furthermore, the example problems are defined by means of a small number of parameters and can be verified easily by other researchers. The method has been applied to real-life 3D problems, which have been presented by Gerstmayr and Schöberl [15].

2 Equations of motion

The equations of motion for large deformations including large strains are derived from Hamilton's principle

$$\delta \int_{t1}^{t2} L dt = 0 \tag{1}$$

where L is the Lagrange functional $L = T - V$. The kinetic energy reads

$$T = 1/2 \int_{V_0} \rho |\dot{u}|^2 \, dV_0. \tag{2}$$

Here, $\dot{u}$ is the absolute velocity (measured from an inertial frame) in every point of the reference volume V_0. For the present case of absolute coordinates, which means that u depends linearly on the degrees of freedom, the variation of T leads to a constant mass matrix. Note that in the case of the FFRF, the displacement u is a nonlinear function of the unknown rigid body displacements and unknown small deformations. We assume linear material behavior and no follower forces, therefore the variation of the potential energy is equal to the virtual work of internal forces and the virtual work of boundary and volume forces

$$-\delta V = -\int_{V_0} S : \delta E \, dV_0 + \int_{V_0} f_0 \cdot \delta u \, dV_0 + \int_{A_0} t_0 \cdot \delta u \, dA_0, \tag{3}$$

where S denotes the 2^{nd} Piola-Kirchhoff stress tensor, E the Green strain tensor, V_0 the Volume, f_0 the body forces, t_0 the surface forces and u the displacements. The Lagrangian (material) formulation is used throughout, and written in tensorial notation, see e.g. Bonet and Wood [4]. S is defined by means of a hyper-elastic energy functional $W(E)$

$$S = \frac{\partial W(E)}{\partial E}. \tag{4}$$

The abbreviation

$$\delta W_{ext} = \int_{V_0} f_0 \cdot \delta u \, dV_0 + \int_{A_0} t_0 \cdot \delta u \, dA_0 \tag{5}$$

is introduced. Integration by parts leads to the variational formulation

$$\int_{V_0} \rho \ddot{u} \cdot \delta u \, dV_0 + \int_{V_0} S : \delta E \, dV_0 - \delta W_{ext} = 0. \tag{6}$$

The strain energy functional for a St. Venant Kirchhoff material reads

$$W(E) = \frac{\lambda}{2}(\mathrm{tr}E)^2 + \mu |E|^2 \tag{7}$$

with the Lamé coefficients μ and λ, for details and range of application see Bonet and Wood [4]. The Green strain tensor E can be expressed in terms of the displacement-gradient ∇u,

$$E = \frac{1}{2}(\nabla u + \nabla u^T + \nabla u^T \nabla u). \tag{8}$$

A conventional geometrically linear formulation neglects second order terms in ∇u,

$$E_{lin} = \frac{1}{2}\left(\nabla u + \nabla u^T\right). \tag{9}$$

This simplification cannot describe large rotations, since $E_{lin} \neq 0$ for rigid body displacements u. Therefore the large displacement is decomposed into

$$u = u_0 + \tilde{u}, \tag{10}$$

where u_0 represents large rigid body displacements and $\tilde{u}$ is a *small* displacement part. Applying the nabla operator to Eq. (10) gives $\nabla u = \nabla u_0 + \nabla \tilde{u}$. The rigid body displacement consists of a translational and a rotational part

$$u_0(x) = u_t + Rx - x, \tag{11}$$

where u_t is a translation vector and R is a rotation matrix which are both attached to each single body separately. The position of a point of a body in reference configuration is denoted by x. The rotation matrix can be expressed by $R = \nabla u_0 + I$, I is the identity tensor. We restrict our problems to small displacements with respect to the rigid body motion, that means $|\tilde{u}| \ll 1$. With sufficient smoothness we may assume small deformations $|\nabla \tilde{u}| \ll 1$, as well. We then approximate E, by neglecting quadratic terms in $\nabla \tilde{u}$:

$$\begin{aligned} E &= \frac{1}{2}\left[(R + \nabla \tilde{u})^T (R + \nabla \tilde{u}) - I\right] = \frac{1}{2}(\nabla \tilde{u}^T R + R^T \nabla \tilde{u} + \nabla \tilde{u}^T \nabla \tilde{u}) \\ &\approx \widetilde{E} := \frac{1}{2}(\nabla \tilde{u}^T R + R^T \nabla \tilde{u}) = \mathrm{Sym}(R^T \nabla \tilde{u}). \end{aligned} \tag{12}$$

The symmetry operator is defined by $\mathrm{Sym}(A) = \frac{1}{2}(A + A^T)$.

3 Unique decomposition of u

The approximation of $\widetilde{E}$ only holds for small values of $\nabla \tilde{u}$. In the case of the FFRF, a mean-axis-frame is suggested by Schwertassek et al. [30] which is defined by a minimization problem of the deformation in the reference configuration. In the case of absolute coordinates, this minimization problem can be written in the form

$$\text{find } \bar{u}_0 \text{ such that} \quad \frac{1}{V}\int_V (u - \bar{u}_0)^T (u - \bar{u}_0) \, dV = \min \tag{13}$$

with $\bar{u}_0 = \bar{u}_t + \bar{R}x - x$. However, we want an explicit expression for $\bar{R}$, therefore we use the following two relations

$$\int_{V_0} (\bar{u}_0 - u)\, dV_0 = 0 \quad \text{and} \quad \int_{V_0} (\nabla\bar{u}_0 - \nabla u)\; dV_0 = 0 \tag{14}$$

which can be resolved to

$$\bar{u}_t = \frac{1}{V_0}\int_{V_0} u\, dV_0 \quad \text{and} \quad \nabla\bar{u}_0 = \bar{R} - I = \frac{1}{V_0}\int_{V_0} \nabla u\, dV_0. \tag{15}$$

This means that we compute the average displacement of u for $\bar{u}_t$ and the average gradient of u for $\bar{R} - I$ instead using a L_2-best approximation of u by an affine linear function $\bar{u}_0$.
The matrix $\bar{R}$ still includes a small amount of the average stretch of the body, therefore a decomposition $\bar{R} = UR$ into a stretch U and a rotation R has to be performed. The decomposition is implemented by applying the deformation $\bar{R}$ to a body and measuring the rotation matrix R due to the deformation of 3 certain points of a body. This decomposition behaves similar to the well known polar decomposition, but it is computationally cheaper.

4 Modeling of Constraints

In 2 and 3 dimensional solid FE formulations the modeling of constraints is still a field of ongoing research. Constraints can represent complicated types of bearings, in certain fields of interest one may even not neglect the lubrication gap or the dynamics of the oil film. However, in many simulations bearings may be simplified. For example, a revolute joint can be modeled by restricting a set of points to lie on a rigid cylinder. In such a formulation, the number of constraints and the complexity of the problem depend on the mesh-size. We therefore use weaker constraint conditions by constraining integral values of the deformation. Let Γ_i denote a part of the surface of a body and $w_i(x)$ a weight function which may be zero (ground joint), constant (spherical joint) or affine linear (cylindrical joints with fixed axis of rotation). We generally define linear constraints as

$$\int_{\Gamma_i} w_i(x) u d\Gamma_i - \int_{\Gamma_j} w_j(x) u d\Gamma_j = 0. \tag{16}$$

For ground joints, w_j is set to zero. Constant values are used for $w_i(x)$ and $w_j(x)$ in order to restrict the distance of the midpoints of two surfaces (rotational joint), affine linear functions are used for $w_i(x)$ and $w_j(x)$ in order to restrict the relative rotation between two surfaces. For the more general case of nonlinear constraints we rewrite the set of constraint equations as

$$B(u) = 0. \tag{17}$$

In the present formulation, constraints are included via Lagrange-parameters, for more details on this modeling, see e.g. [25]. In a mathematically formal way we define the potential of constraint forces

$$V_{pen}(u) = \frac{1}{2\varepsilon}\|B(u)\|^2, \tag{18}$$

where ε is a small parameter. The variation of V_{pen} leads to

$$\delta V_{pen}(u) = \frac{1}{\varepsilon} B(u)^T B'(u)\delta u, \tag{19}$$

where the abbreviation

$$B'(u) = \frac{d}{du}B(u) \tag{20}$$

is used. With the Lagrange parameter $\lambda := \frac{1}{\varepsilon}B(u)$ the weak form of the equations of motion is obtained,

$$\begin{aligned} \int_{V_0} \rho\ddot{u}\cdot\delta u\, dV_0 + \int_{V_0} S : \delta\widetilde{E}\, dV_0 - \delta W_{ext} + (B'(u)^T\lambda)\cdot\delta u &= 0 \\ B(u) &= 0. \end{aligned} \tag{21}$$

5 Variation of the Green strain tensor

In the case of prescribed rigid-body motions, the FE method could be directly applied to Eq. (21). In the more general case of non-prescribed motions of the single bodies, the variation of δR must not be neglected in the variation of the Green strain tensor, Eq. (12). We introduce the abbreviations $G = \nabla u$, $\widetilde{G} = \nabla \tilde{u}$ and make use of the special property of the rotation matrix, $\mathrm{Sym}(R^T \delta R) = 0$. The approximate Green strain tensor (12) is rewritten in the form $\widetilde{E} = \mathrm{Sym}(R^T \widetilde{G})$ and its variation becomes

$$\begin{aligned} \delta\widetilde{E} &= \mathrm{Sym}(R^T \delta\widetilde{G} + \delta R^T \widetilde{G}) \\ &= \mathrm{Sym}(R^T(\delta G - \delta R) + \delta R^T \widetilde{G}) \\ &= \mathrm{Sym}(R^T \delta G + \delta R^T \widetilde{G}). \end{aligned} \tag{22}$$

The dependency $\delta\bar{R}$ on u can be derived from Eq. (15) which gives

$$\delta\bar{R} = \frac{1}{V}\int_V \nabla\delta u \, dV. \tag{23}$$

The variation for R then may be written as

$$\delta R = \frac{\partial R}{\partial \bar{R}} : \delta\bar{R} = \frac{\partial R}{\partial \bar{R}} : \frac{1}{V}\int_V \delta G dV. \tag{24}$$

The dependency $\partial R/\partial\bar{R}$ is computed by means of numerical differentiation. Neglecting the variation of R would mean to neglect a part of the coupling between R and u, resulting in the violation of the conservation of energy. This leads to acceptable results for very small deformations but to instability for moderately small deformations. However, the fact that the change of R and the influence of δR is small leads to an iterative scheme which is computationally efficient but includes all the terms in R.
We introduce the 4^{th} order material tensor $D = \lambda I \otimes I + 2\mu\mathcal{I}$ and the 4^{th} order identity tensor $\mathcal{I}$. The partial derivative of Eq. (7) with respect to the approximated Green strain tensor $\widetilde{E}$ follows to

$$S = \frac{\partial W}{\partial \widetilde{E}} = \lambda \mathrm{tr}(\widetilde{E}) I + 2\mu\widetilde{E} = \widetilde{E} : D. \tag{25}$$

By use of Eq. (22) the variation of the potential of internal forces follows to

$$\int_{V_0} S : \delta\widetilde{E} \, dV_0 = \int_{V_0} \mathrm{Sym}(R^T\widetilde{G}) : D : \mathrm{Sym}(\delta G^T R + \widetilde{G}^T \delta R) \, dV_0. \tag{26}$$

6 Discretized Equations

The main part of the internal energy (26) can be rewritten in the following discretized form

$$\int_{V_0} \mathrm{Sym}\left(R^T\widetilde{G}\right) : D : \mathrm{Sym}\left(\delta G^T R\right) \, dV_0 \rightarrow \tilde{u}_h^T R_h^T A R_h \delta u, \tag{27}$$

where the index h indicates that these are discretized terms according to the continuous terms. A is the stiffness matrix of the system in reference configuration. The remaining terms due to δR lead to small quadratic terms with respect to the small displacement $\tilde{u}_h$ and are therefore placed at the right hand side of the resulting equations

$$\int_{V_0} \mathrm{Sym}\left(R^T\widetilde{G}\right) : D : \mathrm{Sym}\left(\widetilde{G}^T\delta R\right) \, dV_0 \rightarrow f_{\delta R}(\tilde{u}_h^2)\delta u. \tag{28}$$

The FE discretization leads to a system of differential-algebraic equations (DAEs)

$$\begin{aligned} M\ddot{u}_h + R_h^T A R_h \tilde{u}_h + B_h'(u_h)^T \lambda_h &= f_h + f_{\delta R} \\ B_h(u_h) &= 0. \end{aligned}$$

The right hand side only depends on external forces and on terms which result due to δR. Additionally we introduce $f_0 = (R_h^T A R_h) u_0$ and $\bar{f} = f_h + f_{\delta R} + f_0$. Applying the matrix R_h to the first equation we get

$$\begin{aligned} M R_h \ddot{u}_h + A R_h u_h + R_h B_h'(u_h)^T \lambda_h = &\quad R_h \bar{f} \\ B_h(u_h) = &\quad 0. \end{aligned} \tag{29}$$

We assume linear constraints and split into $B_h(u) = B_1 B_2 u$ where B_1 is only a small matrix depending on the number of constraints and B_2 is a block-diagonal matrix which commutes with R_h and fulfills $B_h R_h^T R_h u = B_1 R_h^T B_2 u R_h$.

7 Integration-scheme

The numerical time–integration scheme is sketched by applying exemplarily the trapezoidal rule. For a linear mechanical system $M\ddot{u} + Au = f$ it reads

$$\begin{aligned} M a_{j+1} + K\left[u_j + \tau v_j + \tfrac{\tau^2}{4}(a_j + a_{j+1})\right] &= f_{j+1}, \\ u_{j+1} = u_j + \tau v_j + \tfrac{\tau^2}{4}(a_j + a_{j+1}), \quad v_{j+1} &= v_j + \tfrac{\tau}{2}(a_j + a_{j+1}) \end{aligned} \tag{30}$$

where τ is the time-step size, the velocities are denoted by $v = \dot{u}$ and the accelerations are $a = \ddot{u}$. The index j indicates the previous and the index $j+1$ the actual time step. Only in the first line, a system of equations needs to be solved while the second line is just evaluated. We put terms with index j to the right hand side and rewrite our system as

$$\begin{array}{rcccc} (M + \tau^2 A) R_h a & + & B_2^T R_h B_1^T \lambda & = & R_h \bar{f} + d, \\ B_1 R_h^T B_2 R_h a & & & = & e. \end{array} \tag{31}$$

This system can be solved efficiently: We eliminate $R_h a$ and get the Schur-complement equation

$$B_1 R_h^T B_2 (M + \frac{\tau^2}{4} A)^{-1} B_2^T R_h B_1 \lambda_h = B_1 R_h^T B_2 (M + \tau^2 A)^{-1} (R_h \bar{f} + d) + e. \tag{32}$$

The matrix $B_2(M + \tau^2 A)^{-1} B_2^T$ is computed for certain time stepsizes τ only once for the whole simulation. Thus, the computationally costly part of the solution is computed in advance.

7.1 Implementation of the integration scheme

The DAE-system Eq. (29) is of index 3. According to Hairer et al. [19] we may apply certain kinds of Runge-Kutta methods like the RadauIIA method with $s \geq 2$, s denoting the number of stages of the Runge-Kutta method. The order of convergence for the algebraic variable is the highest for the investigated Runge-Kutta schemes with $s - 1$.
In the subsequent examples the 2 and 3-stage RadauIIA formula has been applied successfully. The above described method for the decomposition of the system in a constant and a time-dependent part easily works for 1-stage integration methods but is cumbersome for methods with several stages. For the sake of simplicity, a modified Newton method is used. For small time steps the Jacobian of a method with n-stages approximates the Jacobian of a method using n steps with a 1-stage method. We therefore only compute the residual of the chosen n-stage method but we use the Jacobian of the trapezoidal rule for every n stages.

8 Numerical example: 3D pendulum

In the following example, a beam-type formulation is compared with the present formulation studying plane motions of a pendulum released from the horizontal position. The pendulum only may rotate around its

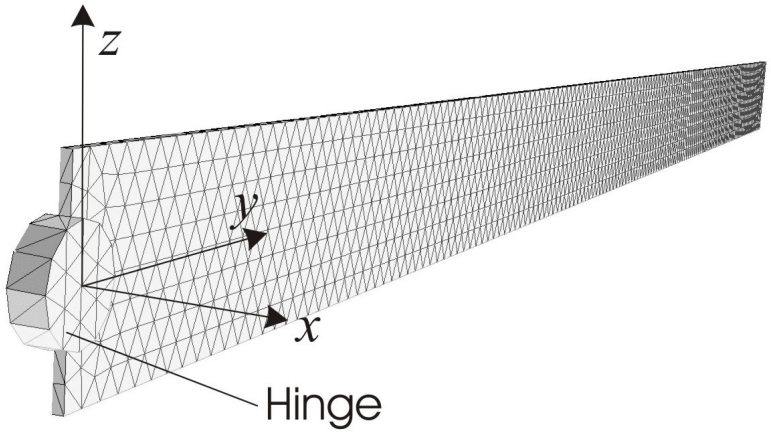

Figure 1: Mesh of the 3-D model of the pendulum.

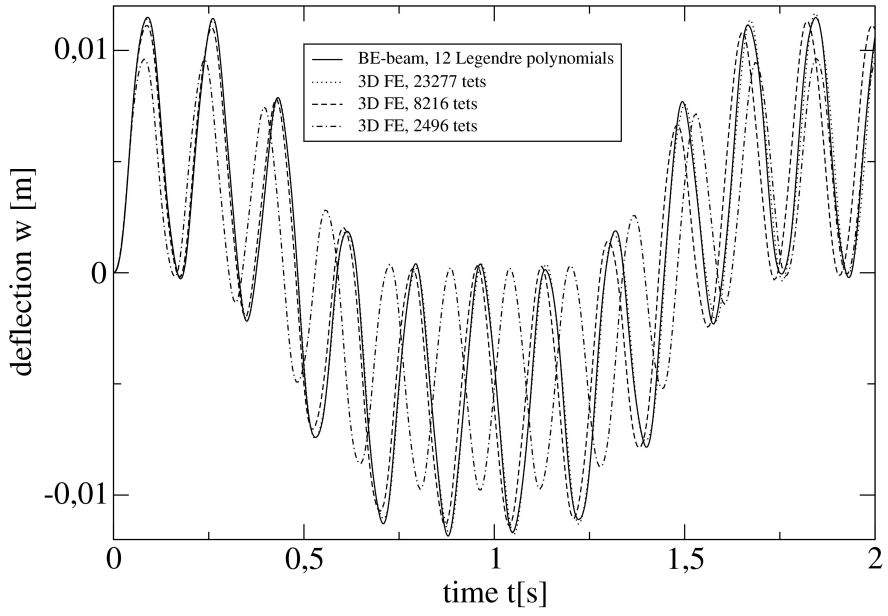

Figure 2: Comparison of a pendulum, midspan-deflection.

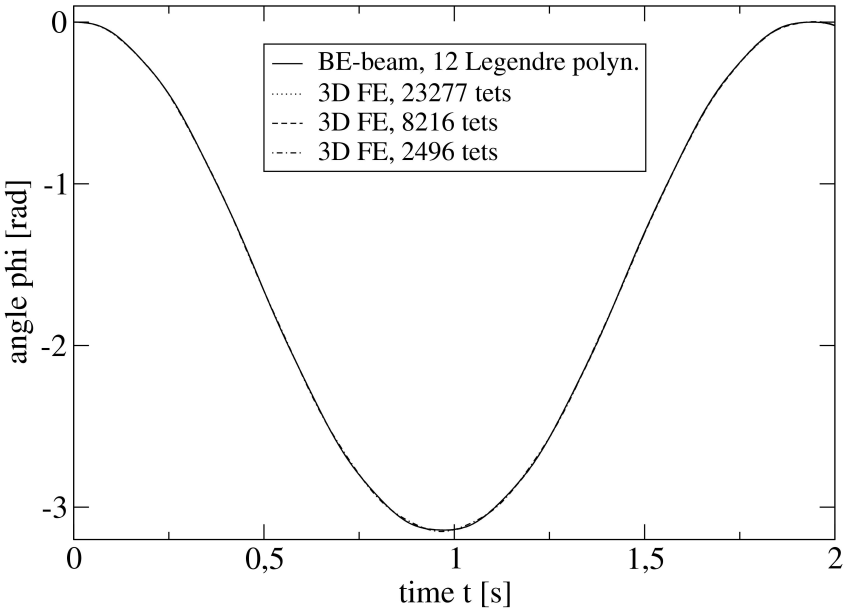

Figure 3: Comparison of pendulum, rigid-body angle.

x-axis, see Figure 1. The geometrical parameters of the example are chosen such that it is comparable to a conventional beam formulation, because there is no other formulation available for the authors in order to compare the results. The pendulum has a length of 1m and a rectangular cross-section with a height of 50mm and a width 2.5mm. The pendulum is very thin in order to reduce the number of elements for the total model and to get a converged solution for the deflection. Young's modulus has been chosen as $2.1 \cdot 10^8$ and Poisson's ratio is 0.3. The influence of the hinge with respect to the angular velocity or deflection is negligible. The rigid-body angle is defined as the angle between the horizontal axis and the line defined by the support and the end-point of the pendulum.
The present formulation is compared with a FFRF where the pendulum is modeled by means of the Bernoulli-Euler beam theory. Small deformations but large rotations are taken into account, for details of the study see Dibold [7]. The problem is discretized in space by the Ritz-method, where 12 Legendre polynomials are used for the modeling of the deflection of the whole pendulum. A comparison between 8, 10 and 12 shape functions showed that the solution was already converged.
The present method has been implemented into the extendable FE-code NGSolve, which is part of the program NETGEN/NGSolve. Tetrahedral elements with quadratic shape functions have been used for the present study. The support is realized by a very thin cylinder attached to the pendulum. The mesh of the model (showing the support) is depicted in Figure 1. The midpoints of both sides of the cylinder are fixed to the ground, meaning that the integral of the displacements at each side has to be zero. The pendulum is released from the horizontal position and driven only due to gravity (g=$9.81 m/s^2$). Figure 3 shows a comparison of the angle of both models which coincide perfectly. Figure 2 shows a comparison of the mid-span deflection of the two models. The deflection is defined as the distance of the deformed axis to the undeformed co-rotated axis, given by the line between the support and the end-point of the beam.

9 Numerical example: slider-crank mechanism

In order to show the functionality of the formulation for a problem with joints between two bodies, a slider-crank mechanism is studied. The mechanism consists of a driving beam which only exhibits rotation and a driven beam which is connected to the driving beam at one end and the other end is restricted to horizontal motion. The dimensions of the driving beam are $L = 0.5$m, $H = 50$mm, $W = 5$mm and of the driven beam

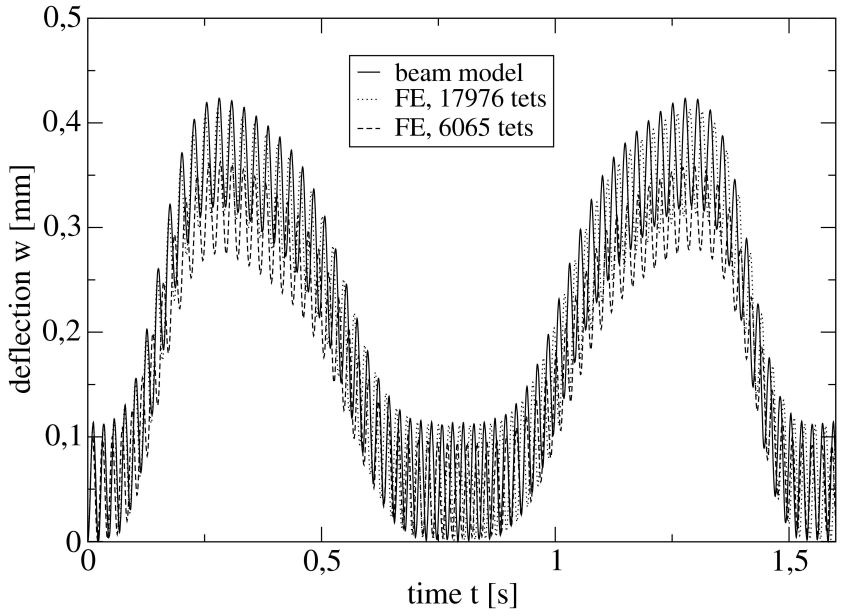

Figure 4: Comparison of a slider-crank mechanism, deflection of driven body.

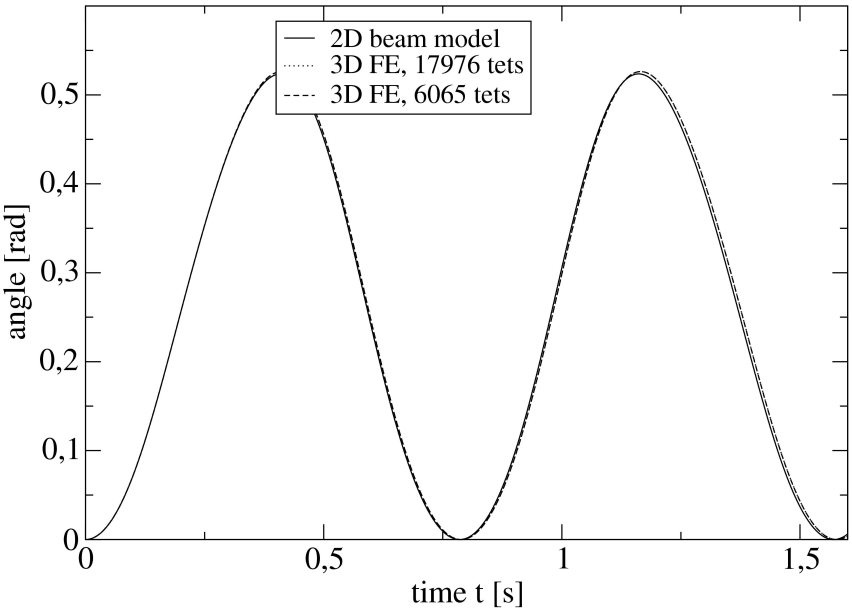

Figure 5: Comparison of a slider-crank mechanism, angle of driven body.

$L = 1$m, $H = 50$mm, $W = 5$mm. Concerning material properties for both beams, Young's modulus is set to $E = 2.1E10$, Poisson's Ratio is $\nu = 0.3$ and density is $\rho = 7800$. The mechanism is driven by its own weight under gravity $g = 9.81m/s$ and is initially in the horizontal position. The total computational time for the problem with the finest mesh (17976 quadratic tetrahedral elements, 6166 points), with the 2-stage RadauIIA time–integration method and 3200 time steps (0.5ms) on a Pentium IV (2.4GHz) computer was 12 hours 15 minutes. The computational time for one time step is therefore 13.8 sec, where a nonlinear problem with approximately 74000 unknowns has to be solved for the two stages of the RadauIIA method. For the approximation of the two-stage method with a one-stage method, ca. 10 iterations are necessary. Explicit methods might compute one time step faster, but they need much smaller time steps in order to get a stable and accurate solution, while in the present implicit method the solution converges for $t = 0.5ms$ and larger time steps (5ms) might be used for an estimation of the solution.
A comparison with a beam-type formulation has been performed according to the this example. The midspan-deflection of the driven beam with respect to a chord-frame is depicted in Figure 4, the rigid body rotation of the driven beam, measured by the angle of the chord-frame is depicted in Figure 5. Both results agree well with the beam theory although a 3-dimensional FE-computation with constraint conditions in integrated form is compared with a 2-dimensional beam-theory.

Acknowledgements

Support of the present work by a grant of the Austrian National Science Fund (FWF) within project P15195-TEC (3D Dynamics of Elasto-Plastic Robots) and within the Start Project grant Y-192 "hp-FEM : Fast Solvers and Adaptivity" is gratefully acknowledged. The authors are grateful to H. Irschik, University of Linz, for valuable discussions with respect to the contents of the present paper.

References

[1] J.A.C. Ambrósio, Geometric and material nonlinear deformations in flexible multibody systems, *Computational Aspects of Nonlinear Structural Systems with Large Rigid Body Motion* (J.A.C. Ambrósio and M. Kleiber, Ed.), Nato Science Series, IOS Press (2001).

[2] J. Argyris. An excursion into large rotations, *Comp. Meth. Appl. Mech. Engrg.*, **32**,85–155, 1982.

[3] T. Belytschko and B.J. Hsieh. Non-linear transient finite element analysis with convected co-ordinates, *Int. J. Num. Meth. in Engrg.*, **7**,255–271, 1973.

[4] J. Bonet, R. D. Wood, *Nonlinear continuum mechanics for finite element analysis*, Cambridge University Press, U.K. (1997).

[5] H. Bremer and F. Pfeiffer, *Elastische Mehrkörpersysteme*, B. G. Teubner, Stuttgart, Germany (1992).

[6] K. E. Brenan, S. L. Campbell, and L. R. Petzold, *Numerical solution of initial-value problems in differential-algebraic equations*, SIAM, Philadelphia (1996).

[7] M. Dibold, Eine Studie zur computerunterstützten Berechnung räumlicher Bewegungen inelastischer Maschinenteile, Master's thesis, University of Linz, Austria, (2002).

[8] J. Pfister, P. Eberhard, *Frictional contact of flexible and rigid bodies* Granular Matter **4**, Springer-Verlag (2002), 25–36.

[9] R.–F. Fung, *Dynamic analysis of the flexible connecting rod of a slider-crank mechanism*, J. Vib. and Acoust., **118** (1996), 687–689.

[10] M. Géradin, A. Cardona, *Flexible multibody dynamics – A finite element approach*, Wiley, New York (2001).

[11] J. Gerstmayr, *A solution strategy for elasto-plastic multibody systems and related problems*, University of Linz, Austria (2001).

[12] J. Gerstmayr, H. Irschik, Vibrations of the elasto-plastic pendulum, Int. J. Nonlin. Mech., **3**8, 111–122, (2003).

[13] J. Gerstmayr. The absolute nodal coordinate formulation with elasto-plastic deformations, In *Proceedings the Multibody Dynamics 2003 conference*, J.A.C. Ambrsio (Ed.), Lisbon, Portugal, 2003.

[14] J. Gerstmayr. Strain tensors in the absolute nodal coordinate and the floating frame of reference formulation, Nonlinear Dynamics **34** (2003) 133–145.

[15] J. Gerstmayr, J. Schöberl, A 3D Finite Element Approach to Flexible Multibody Systems, Proceedings of the Fifth World Congress on Computational Mechanics (WCCM V), Eds.: Mang, H.A.; Rammerstorfer, F.G.; Eberhardsteiner, J., Vienna University of Technology, Vienna, Austria, (2002). http://wccm.tuwien.ac.at

[16] J. Gerstmayr and J. Schöberl. An Implicit Runge-Kutta Based Solver for 3-Dimensional Multibody Systems, *PAMM*, **3**(1),154–155, 2003.

[17] E. Hairer, S. P. Nørsett, and G. Wanner, *Solving ordinary differential equations I, nonstiff problems*, Springer–Verlag Berlin Heidelberg (1987).

[18] E. Hairer and G. Wanner, *Solving ordinary differential equations II, stiff and differential-algebraic problems*, Springer–Verlag Berlin Heidelberg (1991).

[19] E. Hairer and Ch. Lubich, and M. Roche, *The numerical solution of differential-algebraic systems by Runge-Kutta methods*, Lecture Notes in Math. 1409, Springer–Verlag, (1989).

[20] E.J. Haug, *Computer-Aided Kinematics and Dynamics of Mechanical Systems*, Allyn and Bacon, Boston (1989).

[21] J. G. de Jalón and E. Bayo, *Kinematic and dynamic simulation of multibody systems: The real time challenge*, Springer, New York, (1994).

[22] L. Kübler, P. Eberhard, J. Geisler, *Flexible multibody systems with large deformations and nonlinear structural damping using absolute nodal coordinates*, Nonlinear Dynamics **34** (2003) 31–52.

[23] K. Magnus, *Dynamics of multibody systems*, Springer Verlag, Berlin (1978).

[24] P.E. Nikravesh, *Computer-Aided Analysis of Mechanical Systems*, Prentice-Hall (1988).

[25] J. C. G. Orden, J. M. Goicolea, *Conserving properties in Constrained Dynamics of flexible multibody systems*, Multibody Sys. Dyn., **4** (2000), 225–244.

[26] W. Pan and E.J. Haug, *Dynamic simulation of general flexible multibody systems*, Mech. Struct. & Mach. **27** (1999), 217–251.

[27] A.A. Shabana, *Dynamics of multibody systems*, Second Edition, John Wiley & Sons (1998).

[28] W. Schiehlen (ed.), *Multibody system dynamics*, Kluwer Academic Publishers, Netherlands (1997).

[29] R. von Schwerin, *Multibody system simulation; numerical methods, algorithms, and software*, Springer Verlag Berlin (1999).

[30] R. Schwertassek, O. Wallrapp. A. A. Shabana, *Flexible multibody simulation and choice of shape functions*, Nonl. Dyn. **20** (1999), 361–380. Springer Verlag Berlin (1999).

[31] B. Simeon, *Numerische Integration mechanischer Mehrkörpersysteme: Projizierende Deskriptorformen, Algorithmen und Rechenprogramme*, Tech. report, Fortschritt-Berichte VDI, Reihe 20, Nr. 130, VDI Verlag, Düsseldorf, Germany (1994).

[32] J. C. Simo and L. Vu-Quoc, *On the dynamics of flexible beams under large overall motions - the plane case: Part I*, J. Appl. Mech. **53** (1986), 849–863.

[33] J. Wittenburg, *Dynamics of Systems of Rigid Bodies*, Teubner, Stuttgart (1977).

[34] O. C. Zienkiewicz and R. L. Taylor. *The Finite Element Method*, Volume 2 – solid mechanics. Butterworth Heinemann, London, 2000.